

de Haas-van Alphen Effect of FeP in Double Helical Magnetic State

Tatsuhiko NOZUE*, Hisao KOBAYASHI, Noriaki KIMURA¹,
 Haruyoshi AOKI¹ and Takashi KAMIMURA

Department of Physics, Tohoku University, Sendai 980-8578

¹*Center for Low Temperature Science, Tohoku University, Sendai 980-8578*

(Received September 14, 2000)

The de Haas-van Alphen (dHvA) effect has been investigated on high-quality single crystals of FeP in a double helical magnetic state with a $5c$ period in the magnetic fields up to 14 T and at temperatures down to 0.42 K. Single crystals were grown by the chemical transport technique using iodine as the transport agent. Nineteen branches were observed in three crystallographic planes (100), (010) and (001), and analyzed with simple analytic equations for the Fermi surfaces. Many of the dHvA branches have a characteristic angular dependence and are found to correspond to the orbits on surfaces beyond the Brillouin zone in the magnetic state which is reduced to $1/5$ of the non-magnetic one with the MnP-type along the [001] direction. These branches originate from the orbits caused by a magnetic breakdown phenomenon under high fields. Cyclotron mass ratios were obtained to be up to 5.9, whereas the electronic specific heat coefficient is rather small, $2.86 \text{ mJK}^{-2}\text{mol}^{-1}$.

KEYWORDS: FeP, dHvA effect, Fermi surface, magnetic breakdown, cyclotron mass, specific heat

§1. Introduction

For transition metal compounds such as pnictides and chalcogenides, the hybridized electronic states between d electrons of a metal and p electrons of a ligand atom dominate their properties of a crystalline structure, electrical resistivity, magnetism and so on. Among these compounds, the monpnictides have a hexagonal NiAs-type ($P6_3/mmc$) or an orthorhombic MnP-type ($Pnma$) structure in which the atoms are displaced slightly from the atomic position of the NiAs-type. Only Cr, Mn and Fe compounds have a magnetic order.¹⁾ CrSb is an antiferromagnet with a Cr moment of $3.0\mu_B$, and Mn_{1+x}Sb and MnAs ferromagnet with 3.2 and $3.3\mu_B$, respectively, at 4.2 K. These compounds have the NiAs-type structure. On the other hand, MnP, FeP, CrAs and FeAs with the MnP-type have double helical spin arrangements at the ground state. The incommensurate propagation vector is along the [001] direction. Felcher *et al.* showed by neutron diffraction experiments that FeP has the double helices below 125 K with Fe moments of 0.46 and $0.37\mu_B$ which depend on the each helix and a nearly commensurate propagation with a vector, $\mathbf{q} = 0.20 \times \mathbf{c}^*$ at 4.2 K, as shown in Fig. 1.²⁾

It is necessary to reveal the electronic structure of these compounds experimentally on high quality samples to investigate comprehensively their wide variety of magnetic and electric properties. So far, we have measured the de Haas-van Alphen (dHvA) effect on NiAs^{3,4)} with a small-distorted NiAs-type⁵⁾ and on CrP^{6,7)} with the MnP-type structure and discussed the results on the basis of calculated band structures. They are Pauli-paramagnetic with weakly temperature dependent susceptibilities. In CrP, some branches originating from a

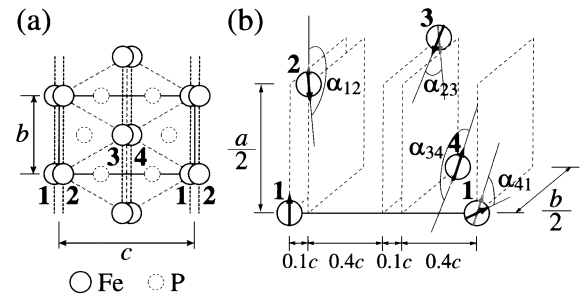


Fig. 1. (a) MnP-type crystal structure as projected on the (100) plane. (b) Double helical spin structure of FeP. The angles between neighbor atoms are $\alpha_{12} = \alpha_{34} = +176^\circ$, $\alpha_{23} = \alpha_{41} = -140^\circ$.

magnetic breakdown phenomenon were observed.⁷⁾ The electron breaks through the crystalline gap in k -space under high fields and makes a large closed orbit which is beyond the band structure calculation.⁸⁾ Such a branch was observed in some substances such as Cr⁹⁾ and Ni_3Al .¹⁰⁾ In chromium, an incommensurate longitudinal spin density wave (SDW) occurs below 123 K.¹¹⁾ The results of the dHvA measurement were interpreted in terms of the chain model.¹²⁾ In this model, the Fermi surfaces consist of the chains along the propagation vector of SDW of nearly ellipsoid surfaces obtained from the calculated band structure in the paramagnetic state. Some branches were caused by the orbits due to magnetic breakdown at the crossing points of the chains. In the dHvA measurement of Ni_3Al which exhibits weakly ferromagnetism below 41 K,¹³⁾ two groups of several close branches were observed. These groups were interpreted in terms of magnetic breakdown between two Fermi surfaces attributed to the bands split by the exchange and the spin-orbit interactions. Among the magnetic transi-

* E-mail: noz@mail.cc.tohoku.ac.jp

tion metal mononictides, the dHvA effect on MnP was measured along the symmetric directions.¹⁴⁾ MnP has the complicated magnetization process dependent on the magnitude and direction of magnetic field.¹⁵⁾ Therefore the topology of Fermi surface was not obtained.

In this paper, we report the results of dHvA effect measurements of FeP crystals and discuss the topology of Fermi surfaces with simple analytic equations. It will be shown that most of the branches correspond to the orbits originating from magnetic breakdown, which is attributed to the superstructure due to the double helical spin order. The cyclotron mass ratios are compared with results obtained presently for some transition metal compounds.

§2. Experimental

Polycrystalline samples were prepared by the following procedure. Appropriate amounts of starting materials Fe rods (99.99% purity) and P flakes (99.9999%) were sealed under vacuum in a silica tube which were progressively heated to 850°C for 3 days, kept at this temperature for 3 days and then cooled slowly to room temperature. The reacted compound was carefully ground and reheated at 850°C for several days in an evacuated silica tube. The lattice constants a , b and c were estimated to be 5.196(1), 3.098(1) and 5.792(1) Å, respectively, at room temperature and agree well with those of the previous works.^{2, 16)} Single crystals were grown by a chemical vapor transport technique using iodine as a transport agent. The powdered sample of about 1 g was sealed in a silica tube with 2 mg cm⁻³ amount of iodine under vacuum at about 77 K to suppress a sublimation of iodine during the evacuation procedure. The silica tube was placed in a furnace in which the charge zone was kept at 815°C and the growth zone at 675°C. After 3 weeks, the tube was cooled slowly to room temperature. The FeP single crystals grew at the growth zone, where the largest one among these single crystals is a size of about 2 × 2 × 3 mm³. The obtained single crystals have an extremely high quality because the residual resistivity is 0.3 μΩ cm and the residual resistivity ratio, $\rho(300\text{ K})/\rho(4.2\text{ K})$, is over 1000, as shown in Fig. 2.

The specific heat measurements were carried out using an adiabatic method with a mechanical heat switch in the temperature range from 1.5 to 30 K and by means of an AC-calorimeter with a heat source of chopped light from 20 K to room temperature. The specific heat data obtained by the AC-calorimeter were normalized to the absolute value determined by the adiabatic method in the temperature range from 20 to 30 K.

The dHvA effect was measured on a cubic single crystalline sample, 1 × 1 × 1 mm³, by a field modulation method in applied magnetic fields up to 14 T at temperatures down to 0.42 K. The field direction was rotated in the three principal crystallographic planes of orthorhombic symmetry, that is, the (100), (010) and (001) planes. The dHvA oscillations in which lower and higher frequencies than about 1000 T were extracted by the Fourier transform analysis were obtained in the field ranges from 6 to 10 T at a rate of 0.2 T/min and from 10 to 14 T at 0.1 T/min, respectively. In the lower field

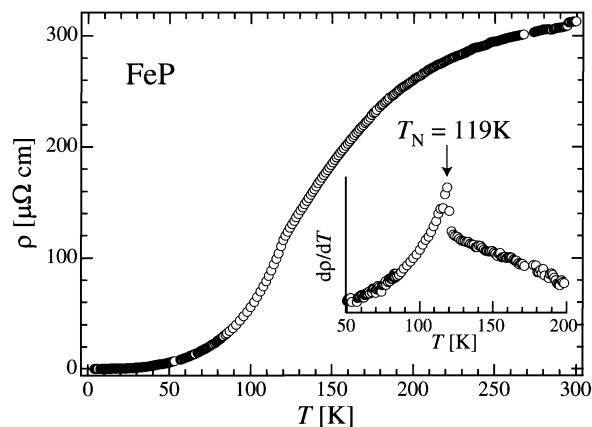


Fig. 2. Temperature dependence of electrical resistivity for a current along the [010] direction in FeP. The curve bends at 119 K where the differential resistivity has a peak as shown in the inset.

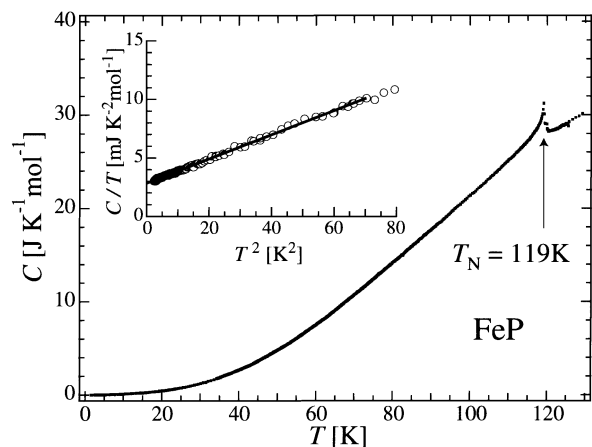


Fig. 3. Temperature dependence of specific heat in FeP. The peak at 119 K originates from the magnetic order. The inset shows the plot of C/T versus T^2 .

range from 6 to 10 T, an AC modulation field, h_0 , was 6.9×10^{-3} T at a frequency 64 Hz and the signals were detected at the fundamental frequency. On the other hand, the signals were detected at the second harmonic with $h_0 = 8.0 \times 10^{-3}$ T at 90 Hz in the higher field range from 10 to 14 T. However, the dHvA oscillation was measured from 1 to 14 T along three symmetric directions. The temperature dependence of dHvA oscillation was measured in the ranges from 0.63 to 1.65 K in the lower field and from 0.42 to 1.56 K in the higher field to obtain the cyclotron mass ratio.

§3. Results

Figure 3 shows the temperature dependence of the specific heat, C . The small but distinct peak at 119 K corresponds to the antiferromagnetic order.²⁾ The entropy change around 119 K is estimated to be $0.2 \text{ J K}^{-1} \text{ mol}^{-1}$ and this small entropy change is attributed to the small ordered moment. As seen in Fig. 2, we have observed an anomaly in the electrical resistivity curve at the same temperature. The electronic specific heat coeffi-

cient is obtained to be $2.86 \text{ mJK}^{-2} \text{ mol}^{-1}$ from the plot as C/T versus T^2 as shown in the inset of Fig. 3, which is comparable with that of Pauli paramagnetic NiAs, $3.01 \text{ mJK}^{-2} \text{ mol}^{-1}$.³⁾

The magnetizations along the symmetric directions, [100], [010] and [001], at 4.2 K were obtained to be proportional to the field up to 5 T, using a SQUID magnetometer. The value at 5 T is as small as 0.5% of the Fe moment obtained by the previous neutron diffraction measurement.²⁾ The susceptibilities along the three directions were estimated to be $1.8 \times 10^{-5} \text{ emu cm}^{-3}$. Since the dHvA signals show the smooth baseline within the range up to 14 T as described below, the magnetization seems to be small even at 14 T. Then we regard the applied field, H , as the magnetic induction, B .

Figure 4 shows a typical dHvA oscillation observed in the field along the [010] direction at 0.45 K. The smooth baseline of the oscillation strongly suggests that no magnetic phase transition takes place up to 14 T. Since the direction of magnetic moments in the double helical magnetic state can be changed by the magnetic field, we have analyzed the dHvA oscillations in four divided regions; from 2.32 to 2.52, from 3.96 to 4.56, from 7.44 to 9.90, and from 9.52 to 13.94 T, which correspond to an equal range in $1/H$. The fundamental dHvA frequencies in the Fourier spectra obtained at the four field ranges are indicated by the arrows, as shown in Fig. 5, and the others were assigned to higher harmonics of the fundamental frequencies and those mixed fundamental ones. As seen in Fig. 5, each fundamental frequency in these four Fourier spectra is considered to be the same value within the experimental accuracy. As the results, the changes of the direction of magnetic moments and the propagation vector induced by the magnetic field are too small to affect the results of dHvA measurements up to 14 T. The independence of the fundamental dHvA frequencies from the magnetic field is different from the results of MnP.¹⁴⁾ This difference is attributed to the small Fe moment and to nearly antiferromagnetic coupling between the nearest-neighbor ferromagnetic-sheets parallel to the (001) plane.²⁾ Thus the magnetic structure of FeP under magnetic field is regarded as the same structure without magnetic field.

A lot of fundamental dHvA frequencies were extracted from the observed dHvA oscillations in the (100), (010) and (001) planes. The angular dependence of these frequencies is shown in Fig. 6 and below 9800 T there are nineteen dHvA branches called by the Greek characters as seen in Fig. 6. The β , ζ , λ , ν , π , ρ , σ , τ and ν branches have minima at the [010] direction. Among

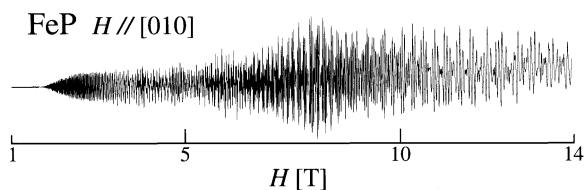


Fig. 4. Typical dHvA oscillation in field along the [010] direction in FeP.

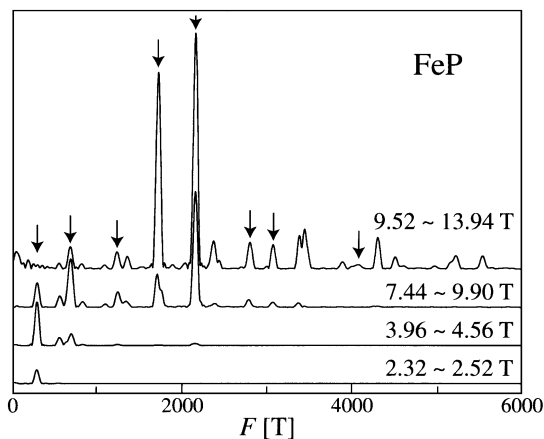


Fig. 5. Fourier spectra of the oscillations in four divided regions along the [010] direction in FeP. Each spectrum consists of fundamental frequencies indicated by the arrows, their higher harmonics and those mixed fundamental ones.

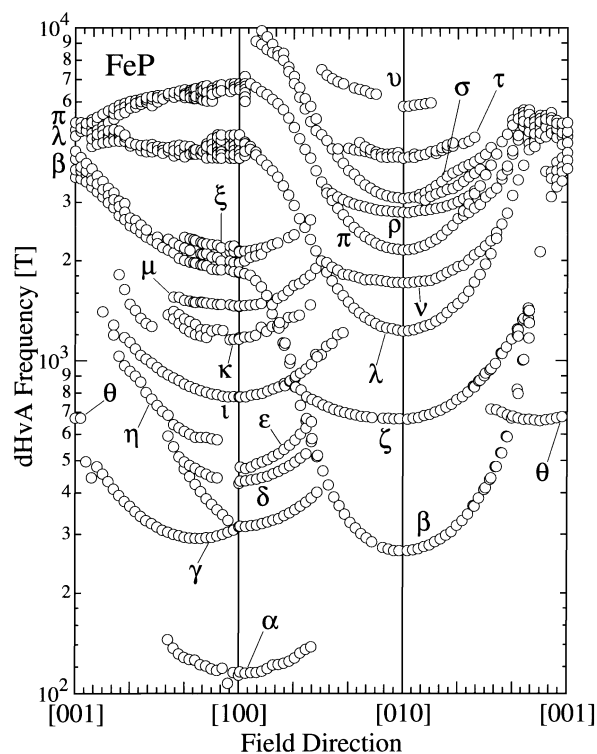


Fig. 6. Angular dependence of the dHvA frequencies in FeP.

these branches, β , λ and π branches were observed in all directions. These branches have the similar angular dependence around the [010] direction. In the (010) plane, they seem to split into several close branches. The ζ , ν and ρ branches were observed between the angles at which the frequencies in these branches are almost equal to those in the β , λ and π branches, respectively, and also have similar angular dependences. Moreover, the σ and τ branches are resemble to π and ρ branches, respectively, though they were observed in limited angular regions. Thus these eight branches are regarded as four sets of the pair branches, that is, (β , ζ), (λ , ν), (π , ρ) and

(σ, τ) .

The α , δ , ι , κ , μ and ξ branches which were observed in the limited angular regions have minima at the [100] direction and have similar angular dependences. The γ branch consists of one frequency in the (010) plane and two frequencies in the (001) plane. The lower branch has the minimum at 24° from the [100] direction in (001). The η and ε were observed only in the (010) and (001) plane, respectively. The θ branch is observed at about 660 T in the angular region from [001] to 42° in (100) and to 3° in (010).

Cyclotron mass ratios, m^*/m_0 , were obtained at the three symmetric directions, [100], [010] and [001]. The linear relation between $\ln(A/T(1 - \exp(-2XT)))$ and T was satisfied within the temperature ranges of this experiment where A is the amplitude of the dHvA oscillation and X is proportional to m^*/m_0 . The obtained m^*/m_0 are summarized in Table I with their dHvA frequencies. The minimum value of m^*/m_0 is 0.60 of the β branch at the [010] direction and the maximum value 5.9 of the λ branch at the [010] direction.

§4. Discussion

Let us consider now Fermi surfaces for the many complicated and characteristic branches as shown in §3. We must take into account the superstructure with a period of $5c$ as discussed below. The band structure of magnetic FeP has not yet been calculated owing to the complicated spin structure. Thus we discussed the observed branches with simple Fermi surfaces drawn by conventional analytic equations.

At first, we take up the β , λ and π branches which were observed in all directions. Thus the Fermi surfaces drawn by these branches are thought to be closed ones at high magnetic field. The closed surface is tentatively considered as an ellipsoid expressed by the equation,

$$\frac{k_x^2}{r_x^2} + \frac{k_y^2}{r_y^2} + \frac{k_z^2}{r_z^2} = 1, \quad (4.1)$$

where x , y and z denote the [100], [010] and [001] direc-

tions, respectively. The parameter r_x is calculated with the frequencies at three symmetric axes, F_x , F_y and F_z , by the relation $r_x = ((2e/\hbar c)(F_y F_z / F_x))^{1/2}$. The parameters of r_y and r_z are expressed by the same relations. As seen in Fig. 6, the value of F_y is much smaller than those of F_x and F_z , each of ellipsoids is found to be elongated along the [010] direction. Around the [010] direction, however, the observed frequencies increase more rapidly than the angular dependence of the branches obtained from the above ellipsoids. Thus the surface around the [010] direction, at least within about 40° from the [010] axis, is considered to be hyperboloidal rather than ellipsoidal. Such the hyperboloid is written as

$$\frac{k_x^2}{r_x^2} - \frac{k_y^2}{r_y^2} + \frac{k_z^2}{r_z^2} = 1. \quad (4.2)$$

As a result, the whole surface for the β , λ and π branches is a ‘‘cocoon’’-like one as shown later. These branches were fitted to the angular dependences of the hyperboloids within about 40° from the [010] direction. Consequently, the radii r_z for the β , λ and π branches were obtained to be 0.072, 0.184 and 0.276 \AA^{-1} , respectively. The Brillouin zone of magnetic FeP is reduced to $1/5 \times (2\pi/c) = 0.217 \text{ \AA}^{-1}$ along the [001] direction, where $(2\pi/c)$ is for the non-magnetic state, that is, for the MnP-type structure. The elliptic orbits for the λ and π branches in the (010) plane are, therefore, beyond the zone boundary perpendicular to the [001] direction. This suggests that the λ and π branches correspond to the large orbits attributed to magnetic breakdown at the zone boundary perpendicular to the [001] direction.

Then we assume a simple elliptic orbit for the π branch in the first Brillouin zone for the non-magnetic state in the (010) plane as shown in Fig. 7(a). In the magnetic state, energy gaps open at which the energy $\varepsilon(\mathbf{k})$ satisfies the relation, $\varepsilon(\mathbf{k}) = \varepsilon(\mathbf{k} + \mathbf{G} \pm n\mathbf{q})$. In this equation, \mathbf{G} is a reciprocal lattice vector and n an integer corresponding to the order of the gap resulting from the interaction with the wave vector \mathbf{q} of the helical magnetic

Table I. dHvA frequencies, F , and cyclotron mass ratios, m^*/m_0 , at the symmetric directions in FeP.

		F (T)	(m^*/m_0)		F (T)	(m^*/m_0)		
[100]	α	115	1.1	[010]	β	270	0.60	
	γ	317	1.5		ζ	670	1.2	
	ι	810	2.3		λ	1216	0.89	
	κ	1180	3.0		ν	1710	1.7	
	μ	1460	2.9		π	2150	1.2	
	β	1840	2.6		ρ	2800	2.3	
		1990	3.5		σ	3070	1.8	
	ξ	2170	3.8		τ	4070	5.1	
	λ	4060	3.1					
		4160	4.2		[001]	θ	660	3.1
		4280	4.5			β	3790	3.7
		4430	5.0				4000	4.0
		4580	5.5				4230	5.0
		4770	5.2			π	4520	5.2
	6530	5.4		4730		5.1		
π		6640	5.7		4880	4.0		
		6790	5.8	λ	5200	5.9		

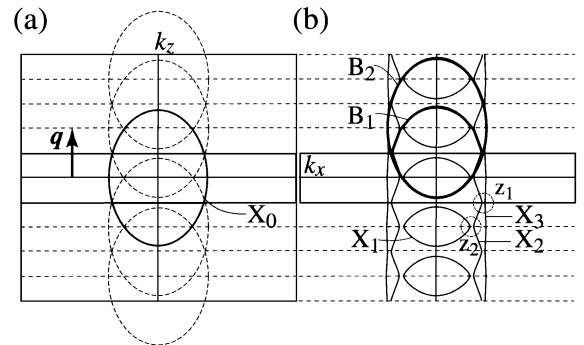


Fig. 7. (a) Orbit X_0 is displaced to the broken ellipses by \mathbf{q} of the double helical spin structure in the Brillouin zone indicated as an outer rectangle. The Brillouin zone is reduced by \mathbf{q} as indicated by the bold rectangle. The ellipse X_0 has the radii r_x and r_z obtained from fitting the π branch around the [010] to the hyperboloidal Fermi surface. (b) Closed orbit X_1 and two open tubular orbits X_2 and X_3 . The possible orbits with magnetic breakdown at the z_1 and z_2 points are indicated as bold ellipses B_1 and B_2 .

order. In Fig. 7(a), the ellipses displaced by $\pm\mathbf{q}$ and $\pm 2\mathbf{q}$ are also shown. As shown in Fig. 7(b), the splits of orbits in the magnetic state arise at the points z_1 and z_2 , and there appear one closed orbit, X_1 , and two tubular open orbits, X_2 and X_3 . Since a gap energy like this origin is generally thought to be very small, magnetic breakdown easily takes place between these orbits. In this case, the possible closed orbit with magnetic breakdown is an orbit B_1 ; $X_1X_2X_1X_2X_1$, which has four times of tunneling at the point z_1 . The other is an orbit B_2 ; $X_1X_2X_3X_2X_1X_2X_3X_2X_1$, which has four times of tunneling at both the points z_1 and z_2 . The larger orbits than the B_2 orbit are also possible to be observed owing to further many times of magnetic breakdown. Furthermore, the areas enclosed with the orbits, X_1 , B_1 and B_2 , are almost equal to those of the β , λ and π frequencies at the [010] direction, respectively. Therefore, these branches come from the close related Fermi surfaces due to magnetic breakdown.

In order to confirm magnetic breakdown mentioned above in this sample, the field dependent amplitude of the dHvA oscillation was analyzed for the β branch for the [010] direction. According to the Lifshitz-Kosevich formula, the field dependent amplitude, A_{LK} , is described as follow,¹⁷⁾

$$A_{LK} \sim H^{-1/2} \frac{\exp(-2\pi^2 k_B T_D / \beta H)}{\sinh(2\pi^2 k_B T / \beta H)}, \quad (4.3)$$

where $\beta = e\hbar/m^*c$ and T_D is the Dingle temperature. In the measurement with the field modulation method, the amplitude of the dHvA signal is obtained to be proportional to A_{AL} multiplied by a Bessel function, $J_k(2\pi F h_0 H^{-2})$. Figure 8 shows the field dependence of the amplitude of β oscillation at the [010] direction. The fitted result for the amplitude to eq. (4.3) below 2 T is shown by the broken curve in Fig. 8, where magnetic breakdown is ignored. Then T_D is estimated to be 0.47 K using $F = 270$ T, $m^*/m_0 = 0.6$, $T = 0.65$ K and $h_0 = 9.8 \times 10^{-3}$ T. As seen in Fig. 8, the broken curve

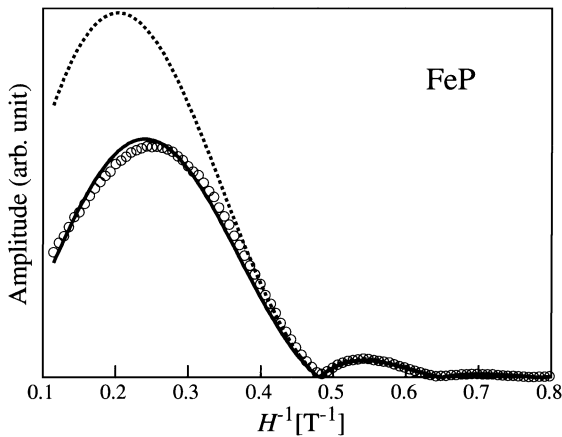


Fig. 8. Field dependence of the amplitude of β oscillation. The broken curve is calculated using eq. (4.3) multiplied by the first order Bessel function, $J_1(2\pi F h_0 H^{-2})$. The solid curve shows the result with the reduction factor R_{MB} due to magnetic breakdown.

deviates from the data points in the high field region. Therefore, the reduction of amplitude due to magnetic breakdown in high field must be taken into account.

If two neighbor orbits are separated by a small gap at a point in k -space, the electron tunnel through the gap with a probability, P , given by $\exp(-H_0/H)$ and is reflected at the point with a probability, Q , given by $(1 - \exp(-H_0/H))$, where the breakdown field, H_0 , depends on the local geometry of both the orbits near the point of tunneling or reflection.¹⁸⁾ The oscillation amplitude is multiplied by the reduction factor written as follow,

$$R_{MB} = P^{n_1/2} Q^{n_2/2}, \quad (4.4)$$

where n_1 is the number of the point at which the tunneling takes place between the relevant orbits and n_2 at which the reflection occurs. Since the β branch originates from the X_1 orbit as shown in Fig. 7(b) and the electron on the orbit was with no tunneling and with reflecting at the two points z_2 , then n_1 and n_2 are 0 and 2, respectively. Thus R_{MB} decreases with decreasing the probability of the reflection at the point z_2 , that is, with increasing the probability of tunneling to the X_2 orbit, in the high field region. The resultant formula of eq. (4.3) multiplied by R_{MB} is fitted to the data obtained with the fixed T_D determined above. The fitted curve is shown by the solid one in Fig. 8 and agrees well with the experimental data. Then H_0 is obtained to be 4.8 T.

As pointed out in §3, the π and ρ branches are considered to be paired ones, that is, they are considered to originate from the different orbits on one ‘‘cocoon’’-like Fermi surface as shown in Fig. 9. The central thin orbit on the surface is assumed to correspond to the π branch and to be hyperboloidal described as eq. (4.2) and two thick orbits at the both ends of surface to the ρ branch and to be ellipsoidal as eq. (4.1). The (β, ζ) and (λ, ν) pair branches on the similar ‘‘cocoon’’-like surfaces have the same relation to the (π, ρ) pair as shown in Fig. 9. To verify the above model, using the fitted parameter r_x, r_y and r_z for the π branch as a hyperboloid and the ρ branch as an ellipsoid, angular dependent frequencies of (β, ζ) and (λ, ν) branches were calculated within the

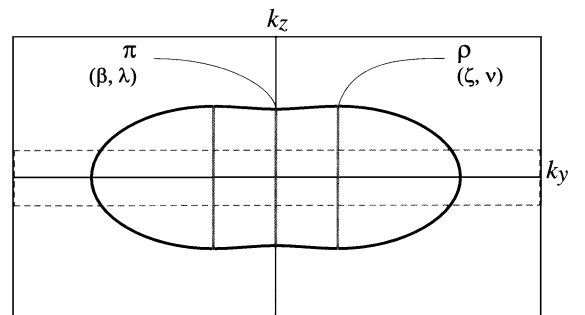


Fig. 9. Model of a ‘‘cocoon’’-like Fermi surface corresponding to (π, ρ) paired branches as projected on the (100) plane. The central thin part corresponds to the π branch and the thick part at the both ends to the ρ branch. The broken rectangle indicates the Brillouin zone in magnetic state. The (β, ζ) and (λ, ν) paired branches are obtained from the similar surfaces with the different dimensions as shown in Fig. 7(b).

angular region of about 40° from the $[010]$ direction in the (001) and (100) planes. The dimensions r_{nx} and r_{nz} in the (010) plane are determined by the relation as follows,

$$\begin{aligned} r_{nz} &= r_z - \frac{nq}{2} \\ r_{nx} &= r_x \left(1 - \left(\frac{nq}{2r_z} \right)^2 \right)^{1/2}, \end{aligned} \quad (4.5)$$

where $n=1$ and 2 correspond to the (β, ζ) and (λ, ν) pair branches, respectively. As shown in Fig. 10, the calculated results were drawn with solid and broken curves which agree with the experimental data qualitatively. Furthermore, as shown in Fig. 10, the σ and τ branches are partly agree with the calculated results using the reverse process. However, the ν branch is not explained with this model.

Subsequently, we discuss the α , δ , ι , κ , μ and ξ branches observed around the $[100]$ direction. They are also similar to each other and, therefore, can be analyzed using the same model with magnetic breakdown mentioned above. In this case, the parameters r_z of the ellipsoids fitted to these branches are also beyond the Brillouin zone in magnetic state, except for the α and δ branches. The angular dependence of the ellipsoids with r_{ny} and r_{nz} calculated from r_x , r_y and r_z of the μ and ξ branches with eq. (4.5) are shown by the solid and broken curves, respectively, in Fig. 11. The broken curves calculated from the ξ branch for $n=1$ and 2 agree well with the κ and α branches, respectively. The solid curve

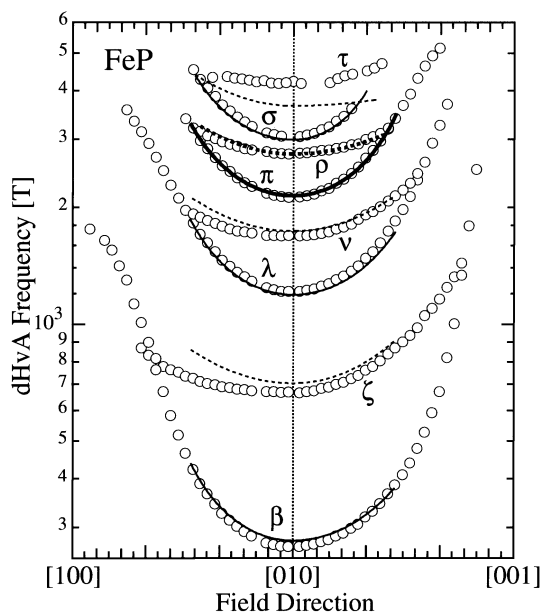


Fig. 10. dHvA branches around the $[010]$ direction in FeP. The bold solid and broken curves show the results of fitting the π branch to the hyperboloidal surface and the ρ branch to the ellipsoid, respectively. The solid curves indicate the angular dependence with the parameter r_{nx} and r_{nz} calculated for $n = 1$ and 2 from the values of r_x , r_y and r_z of the π branch with eq. (4.5). The broken curves indicate the angular dependence calculated from the parameters of the ρ branches in the same way.

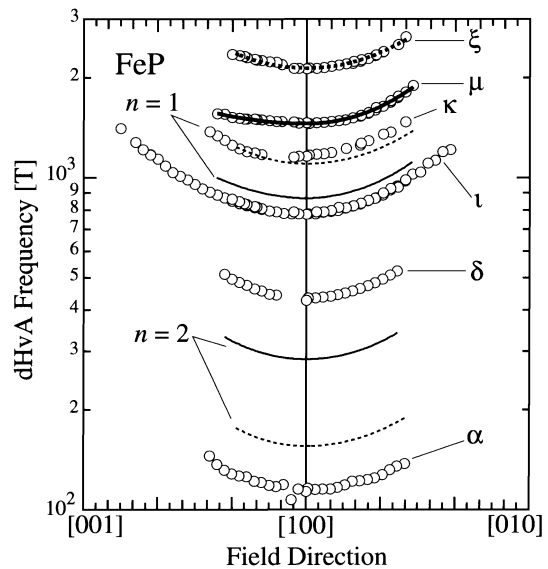


Fig. 11. dHvA branches around the $[100]$ direction in FeP. The bold solid and broken curves show the results of fitting the μ and ξ branches to the angular dependence of the ellipsoidal cross section, respectively. The thin solid and bold curves indicate the angular dependence with the radii of r_{nx} and r_{nz} calculated for $n = 1$ and 2 from the values of r_x , r_y and r_z of the μ and ξ branch with eq. (4.5), respectively.

obtained from the μ branch for $n=1$ agrees qualitatively with the ι branch. The solid curve for $n=2$ disagrees with the observed branches, therefore, the δ branch is thought to be caused by the different origin. Moreover, the γ , ε , η and θ branches are remained to be explained. So far, the Fermi surfaces are considered to be centered in the Brillouin zone. The information about the positions of surfaces was not obtained in this experiment.

As seen in Fig. 6, there observed the β , λ and π branches split into $3\sim 7$ branches for the all directions in the (010) plane. The ζ and ν branches were shown as one branch in Fig. 6 because of the low resolution of the Fourier analysis in the narrow field ranges. However, the ζ and ν oscillations for the $[010]$ direction observed in the wide field range of 1 to 14 T split into three frequencies. The similar branches with a small splitting were observed in chromium⁹⁾ which has an incommensurate longitudinal SDW below 123 K.¹¹⁾ Reifenberger *et al.*¹²⁾ has proposed the chain model, that is, the split branches were attributed to the segment between the intersections of ellipsoidal Fermi surfaces displaced by the incommensurate propagation vector multiplied by an integer. These results suggest that FeP has an incommensurate helical spin structure with the slightly deviated period from $5c$.

Figure 12 presents the plot of the cyclotron mass ratios versus dHvA frequencies for FeP and the other transition metal compounds.^{4, 6, 10, 19-22, 24, 25)} The cyclotron masses of MnSi are strongly enhanced by the low frequency fluctuation of the spin density.²⁶⁾ In AuSn, nearly free electron model is adopted for the s and p electrons, and thus the cyclotron mass ratio is rather small.²⁵⁾ As seen in this figure, FeP has relatively heavy cyclotron masses among the transition metal compounds. However, the electronic specific heat coefficient is rather

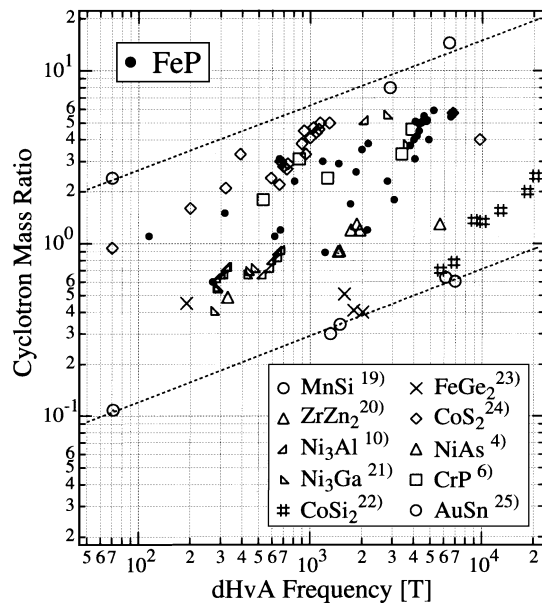


Fig. 12. Cyclotron mass ratio versus dHvA frequency for FeP and the other transition metal compounds. The upper and lower broken lines are to guide the reader's eye.

small, $2.86 \text{ mJK}^{-2} \text{ mol}^{-1}$, which is comparable to that of Pauli paramagnetic NiAs, $3.03 \text{ mJK}^{-2} \text{ mol}^{-1}$,⁴⁾ and considerably smaller than that of Pauli paramagnetic CrP with slightly temperature dependent susceptibility, $8.71 \text{ mJK}^{-2} \text{ mol}^{-1}$.⁷⁾

§5. Conclusion

High quality single crystals of FeP were prepared by the chemical transport reactions, using iodine as the transport agent. On these samples, the dHvA effect was measured in the field up to 14 T at temperature down to 0.42 K. Nineteen branches are assigned in the three principal planes. Four pairs of branches observed around the [010] direction have a similar angular dependence to each other. It was found that the pair branches of the lowest frequency among them correspond to the orbits on surface in the first Brillouin zone reduced by the long period spin structure and the other originates from the larger orbits with several times of magnetic breakdown. The branches around the [100] direction are thought to be in the same situation. The occurrence of magnetic breakdown in this sample is examined with the analysis of field dependent amplitude of the β oscillation at the [010] direction. As shown in Fig. 6, the β , λ and π branches split into several branches in the (010) plane, however, suggest the incommensurate spin structure with a slightly

deviated period from $5c$. The cyclotron mass ratios of FeP are relatively heavy among the transition metal compounds.

Acknowledgments

We are grateful to Profs. T. Suzuki and K. Motizuki for their valuable discussion and encouragement. We wish to thank Dr. M. Matsuura for his kind support to utilize the AC-calorimeter. The present work is supported, in part, by the REIMEI Research Resources of Japan Atomic Energy Research Institute.

- 1) Adachi and Ogawa: *Landolt-Börnstein New Series*, ed. Wijn (Springer-Verlag, 1990) Vol. III/27a p. 148.
- 2) G. P. Felcher, F. A. Smith, D. Bellavance and A. Wold: *Phys. Rev. B* **3** (1971) 3046.
- 3) T. Nozue, H. Kobayashi, M. Sato, A. Uesawa, T. Suzuki and T. Kamimura: *Physica B* **237** (1998) 174.
- 4) T. Nozue, H. Kobayashi, T. Kamimura, T. Kawakami, H. Harima and K. Motizuki: *J. Phys. Soc. Jpn.* **68** (1999) 2067.
- 5) R. Vincent and R. L. Withers: *Phil. Mag. Lett.* **56** (1987) 57.
- 6) T. Nozue, H. Kobayashi, T. Suzuki, H. Yamagami and T. Kamimura: *J. Magn. Soc. Jpn.* **23** (1999) 430.
- 7) T. Nozue, H. Kobayashi, H. Yamagami and T. Kamimura: to be published.
- 8) M. G. Priestley: *Proc. Roy. Soc. A* **276** (1963) 258.
- 9) J. E. Graebner and J. A. Marcus: *Phys. Rev.* **175** (1968) 659.
- 10) T. I. Sigfusson, N. R. Bernhoeft and G. G. Lonzarich: *J. Phys. F: Met. Phys.* **14** (1984) 2141.
- 11) S. A. Werner, A. Arrott and H. Kendrick: *Phys. Rev.* **155** (1967) 528.
- 12) R. Reifenberger, F. W. Holroyd and E. Fawcett: *J. Low Temp. Phys.* **38** (1980) 421.
- 13) F. R. de Boer, C. J. Schinkel, J. Biesterbos and S. Proost: *J. Appl. Phys.* **40** (1969) 1049.
- 14) M. Ohbayashi, T. Komatsubara and E. Hirahara: *J. Phys. Soc. Jpn.* **40** (1976) 1088.
- 15) G. P. Felcher: *J. Appl. Phys.* **37** (1966) 1056.
- 16) K. Selte and A. Kjekshus: *Acta Chem. Scand.* **26** (1972) 1276.
- 17) D. Shoenberg: *Magnetic oscillations in metals* (Cambridge Univ. Press, 1984).
- 18) R. G. Chambers: *Proc. Phys. Soc.* **88** (1966) 701.
- 19) L. Taillefer, G. G. Lonzarich and P. Strange: *J. Magn. Magn. Mater.* **54–57** (1986) 957.
- 20) P. G. Mattocks and A. E. Dixon: *J. Phys. F: Met. Phys.* **11** (1981) L147.
- 21) S. M. Hayden, G. G. Lonzarich and H. L. Skriver: *Phys. Rev. B* **33** (1986) 4977.
- 22) G. C. F. Newcombe and G. G. Lonzarich: *Phys. Rev. B* **37** (1988) 10619.
- 23) I. V. Svecckarev, E. Fawcett and F. W. Holroyd: *Solid State Commun.* **35** (1980) 297.
- 24) A. Ishiguro, A. Sawada, M. Suzuki, H. Hiraka, K. Yamada, Y. Endoh and T. Komatsubara: *J. Magn. Magn. Mater.* **177–181** (1998) 1355.
- 25) G. J. Edwards, M. Spingford and Y. Saito: *J. Phys. Chem. Solids* **30** (1969) 2527.
- 26) G. G. Lonzarich: *J. Magn. Magn. Mater.* **76–77** (1988) 1.